International Journal of Engineering Research & Technology (IJERT)
ISSN: 2278-0181
Vol. 1 Issue 7, September - 2012

Input Power Factor Improvement for Matrix Converter using Direct-SVM Based

Malgireddy Ravi, Technical. Manager, BluevegaSolutions Pvt.Ltd, Hyderabad 500060,
Palarapu Sravan Kumar, Sr.Asst.Professor Aurora's scientific technological research academy bandlaguda, hyd

***Abstract*—matrix converter requires an input filter to improve the input current quality with low harmoni ccomponents, as well as to reduce the input voltage distortion supplied to the MC. However, the input filter's characteristic smake the input power factor (IPF) obtained at unity only in the presence of high output loads, and the IPF degrades significantly under light-load conditions.**

In this paper, we propose a new direct space vector modulation (DSVM) method to achieve the required displacement angle between the input voltage and input current of the MC. A new switching strategy is introduced based on the maximum compensated angle. Then, power factor Improved by using the new DSVM method to achieve the maximum IPF are presented, in which compensation algorithm I is based on using the input filter and power supply parameters to estimate the optimal compensated angle. Compensation algorithm II is subsequently proposed using a proportional–integral controller to overcome drawbacks presented in compensation algorithm I. Simulation results are shown to validate the effectiveness of the proposed compensation algorithms.

***Index Terms*—Direct space vector modulation (DSVM) method, input filter, matrix converter (MC).**

I. INTRODUCTION

IN THE PAST two decades, the evolution of power device technology and the development of large-power integrated circuits have revised the direct ac–ac power conversion technologies. These types of converter fulfill all requirements of conventionally used rectifier/dc link/inverter structures and provide efficient ways to convert electric power for motor drives, uninterruptible power supplies, variable-frequency generators, and reactive energy control [1]–[4].

A matrix converter (MC) delivers the following advantages:

1) sinusoidal input and output current waveforms;

2) controllable input power factor (IPF);

3) operations in all four quadrants of the torque–speed plane due to the regenerative capability;

4) high reliability and long life due to the absence of bulky electrolytic capacitors;

5) smaller and lighter design than other regeneration inverters with equivalent power ratings.

Input filter designs for MC guarantee near-unity power factor operation on the power supply side by improving the main input current quality, which has sinusoidal waveforms containing low harmonic components, and by reducing distortion of input voltages that are supplied to the MC module [5], [6]. The presence of input filter in the direct ac–ac power conversion, which has no energy storage, can cause the instability during operations [7]–[11]. In [12] and [13], the input filter design for sliding mode controlled MC considered the maximum allowable displacement angle introduced by the filter and the controllable IPF capability, as well as the ripple presented in capacitor voltages. The authors in [14] proposed an integration of MC with filters that provides lower electromagnetic interference, lower common-mode current, and lower shaft voltage.

However, the basic hardware limitation of the input filter still exists, which results in a displacement angle between input line-to-neutral voltage and input line current at the main power supply. Consequently, the IPF at the power supply could be far from the desired power factor of unity. In particular, in the case of low-output-power condition, the IPF at the power supply would decrease significantly.

In order to overcome this problem, we proposed a new direct space vector modulation (DSVM) method based on the maximum controllable displacement angle between the input current and input voltage of the MC. The new DSVM method was developed by using a new pulse width modulation (PWM) switching pattern which authors already introduced the basic idea succinctly in [15]. In this paper, two IPF compensation METHODS using the new DSVM are proposed to improve the IPF of the MC. First, a compensation algorithm based on the calculation of the optimal compensated angle is analyzed and discussed. This compensation algorithm provides a fast response which allows high IPF achievement. However, the accuracy of this algorithm depends on some of the MC's hardware configuration parameters, including power supply and LC filter values. Subsequently, another compensation algorithm is suggested to overcome the drawbacks presented in the first compensation algorithm. This compensation algorithm is based on a proportional–integral (PI) controller usage for power factor control. Aside from the flexible adjustment capability of the power factor that

this compensation algorithm can provide, its performance is independent on the MC Hardware Configuration.

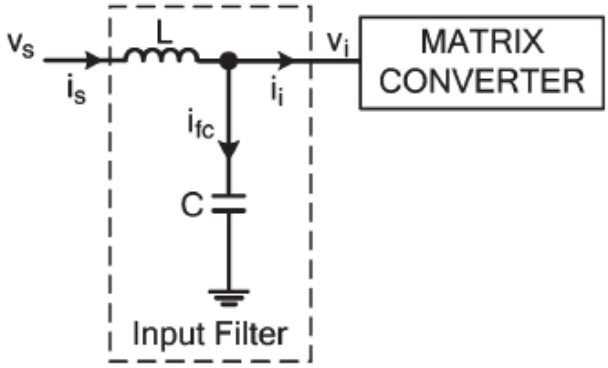

Fig 1. MC equivalent circuit of a single-phase input filter.

Simulation studies are using the proposed theories on a three-phase inductive load (RL) model are conducted. The results obtained are presented illustrating better performances of the proposed compensation algorithms using the new DSVM method. Furthermore, experimental results on a 5-hp induction motor control, applying the power factor compensation algorithm based on a PI controller, are given to validate the feasibility and effectiveness of the proposed compensation algorithms for dynamic load conditions.

II. Input Filter Analysis of MC

The input filter is designed to filter high harmonic components of the input current and to reduce the input voltage distortion supplied to the MC. The following are basic equations regarding input and output voltages, and currents of the MC.

$va = Vm\cos(\omega t)$
$vb = Vm\cos(\omega t - 2\pi/3)$ ..... (1)
$vc = Vm\cos(\omega t - 4\pi/3)$
$V_i = 2(v_a + vbe^{j2\pi/3} + vce^{j4\pi/3})/3 = Vie^{j\alpha i}$ ..... (2)
$V_o = 2(v_A + vbe^{j2\pi/3} + vCe^{j4\pi/3})/3 = Voe^{j\alpha o}$ ..... (3)
$I_i = 2(i_a + ibej2\pi/3 + ice^{j4\pi/3})/3 = Iie^{j\beta i}$ ..... (4)
$I_o = 2(i_A + iBej2\pi/3 + iCe^{j4\pi/3})/3 = Ioe^{j\beta o}$ ..... (5)

From Fig. 1, the following equations are obtained:

$vi = vs - L(dis/dt)$
$ifc = C(dvi/dt)$
$is = ifc + ii.$

Considering the power factor on the power supply side, the power supply frequency in (1) will be taken as the fundamental frequency. The MC control algorithm guarantees the load control requirements and unity power factor at the power supply side as well. Then, (6) can be rewritten as follows:

$$Vs = Vs\, e^{j0}$$
$$Vs = Vs - jwLI_S$$
$$= \frac{\sqrt{VS2 + (WLIS2)}}{1} e^{-Jtan-(wlis/vs)}$$
$$Ii = (1 - w2lc)Is - jwcvs$$

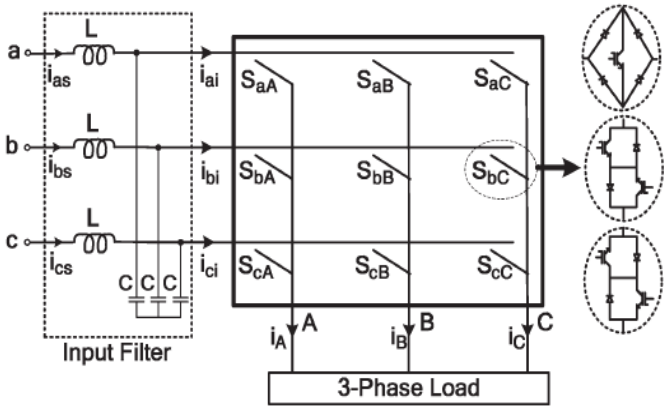

Fig. 2. Structure of a three-phase ac–ac MC.

Finally, the input current of the power supply always leads the input current of the MC with the following displacement angle:

$$\delta = \phi I_S / Ii$$
$$= \tan^{-1}(\omega CVs/(1 - \omega 2LC * Is)$$

From (8), the displacement angle depends on three parameters: the L and C values of the input filter and the fundamental input current amplitude Is, which depends on the output load conditions of the MC. In order to minimize this displacement angle, small LC values are used in the practical MC system.
However, with small LC values, the main power supply current contains higher harmonic components resulting from the wellknown higher cutoff frequency $1/(2\pi\sqrt{LC})$.
To achieve a maximum IPF at the main power supply, the SVM method, which guarantees the input current and input voltage of theMC to be in phase, must be revised to compensate for the displacement angle caused by the input filter.

III. New DSVM Method

A. Space Vectors of MC

The three-phase MC module includes nine bidirectional switches, as shown in Fig. 2. There are 27 possible switching configuration (SC) states. However, only 21 SCs of them can be used to implement the modern control algorithms for the MC such as the SVM and direct torque control methods. As shown in Table I, the following are observed.

1) Group I ($\pm 1, \bullet \pm 2, \ldots, \bullet \pm 9$) consists of the SCs which have two output phases connected to the same input phase.

2) Group II (0_a, 0_b, 0_c) consists of the SCs which have all output phases connected to a common input phase. For each SC, the corresponding line-to-neutral voltage vector and input line current vector have fixed directions as represented in Fig. 3.

3) Group III consists of six other SCs which have the output phases connected to different input phases. The output voltage vector and input current vector have variable directions and can rarely be used.

B. New DSVM Method for MC

For the sake of explaining the new DSVM method, we assume both the desired output voltage and the input voltage space vectors to be located in sector 1 without missing the generality of the analysis ($0 \le \alpha_o \le \pi/3$ and $k_v = 1$, $-\pi/6 \le \alpha_i \le \pi/6$ and $k_i = 1$), as shown in Fig. 3, where k_v and k_i are the output voltage vector sector and the input voltage vector sector, respectively.

Case 1: The displacement angle places the desired input current vector and the input voltage vector in the same sector ($-\pi/6 \le \beta_i \le \pi/6$) in Fig. 3(b). The desired output voltage vector v_o is generated from two vectors V^1_o and V^{11}_o. To match the vector direction as V^{11}_o, among the six possible SCs ($\pm 1, \bullet \pm 2, \ldots, \bullet \pm 9$) that have the output voltage vector in the same direction of V^{11}_o, only two higher voltage magnitude vectors are considered to generate which must maintain the input current vector direction I_i to be inside sector 1 and lag behind the input voltage vector with a certain angle $\delta = \alpha_i - \beta_i$. In order to approach the given conditions, SCs −7 and +9 are selected to drive the MC, and from Fig. 3, the duty ratios of SCs −7 (d_1) and +9 (d_2) should satisfy the following relationship:

$$\begin{cases} \dfrac{d_1}{\sin\left(\frac{\pi}{6}-\beta_i\right)} = \dfrac{d_2}{\sin\left(\frac{\pi}{6}+\beta_i\right)} \\ d_1(-2v_{ab}/3) + d_2(2v_{ca}/3) = v''_o. \end{cases} \quad (9)$$

Solving (9) under the given condition $\delta = \alpha_i - \beta_i$, the duty ratios for SCs −7 and +9 are respectively as follows:

TABLE I
POSSIBLE SCs AND VECTORS USED IN THE MC

	Switching Configurations		Output Voltage		Input Current	
	SC. No.	A B C	V_o	α_o	I_i	β_i
Group I	+1	a b b	$2v_{ab}/3$	0	$2i_A/\sqrt{3}$	$-\pi/6$
	-1	b a a	$-2v_{ab}/3$	0	$-2i_A/\sqrt{3}$	$-\pi/6$
	+2	b c c	$2v_{bc}/3$	0	$2i_A/\sqrt{3}$	$\pi/2$
	-2	c b b	$-2v_{bc}/3$	0	$-2i_A/\sqrt{3}$	$\pi/2$
	+3	c a a	$2v_{ca}/3$	0	$2i_A/\sqrt{3}$	$7\pi/6$
	-3	a c c	$-2v_{ca}/3$	0	$-2i_A/\sqrt{3}$	$7\pi/6$
	+4	b a b	$2v_{ab}/3$	$2\pi/3$	$2i_B/\sqrt{3}$	$-\pi/6$
	-4	a b a	$-2v_{ab}/3$	$2\pi/3$	$-2i_B/\sqrt{3}$	$-\pi/6$
	+5	c b c	$2v_{bc}/3$	$2\pi/3$	$2i_B/\sqrt{3}$	$\pi/2$
	-5	b c b	$-2v_{bc}/3$	$2\pi/3$	$-2i_B/\sqrt{3}$	$\pi/2$
	+6	a c a	$2v_{ca}/3$	$2\pi/3$	$2i_B/\sqrt{3}$	$7\pi/6$
	-6	c a c	$-2v_{ca}/3$	$2\pi/3$	$-2i_B/\sqrt{3}$	$7\pi/6$
	+7	b b a	$2v_{ab}/3$	$4\pi/3$	$2i_C/\sqrt{3}$	$-\pi/6$
	-7	a a b	$-2v_{ab}/3$	$4\pi/3$	$-2i_C/\sqrt{3}$	$-\pi/6$
	+8	c c b	$2v_{bc}/3$	$4\pi/3$	$2i_C/\sqrt{3}$	$\pi/2$
	-8	b b c	$-2v_{bc}/3$	$4\pi/3$	$-2i_C/\sqrt{3}$	$\pi/2$
	+9	a a c	$2v_{ca}/3$	$4\pi/3$	$2i_C/\sqrt{3}$	$7\pi/6$
	-9	c c a	$-2v_{ca}/3$	$4\pi/3$	$-2i_C/\sqrt{3}$	$7\pi/6$
Group II	0_a	a a a	0	x	0	x
	0_b	b b b	0	x	0	x
	0_c	c c c	0	x	0	x
Group III	x_1	a b c	x	x	x	x
	x_2	a c b	x	x	x	x
	x_3	b c a	x	x	x	x
	x_4	b a c	x	x	x	x
	x_5	c a b	x	x	x	x
	x_6	c b a	x	x	x	x

$$d1 = \frac{2q \sin[\alpha o - (kv-1)\pi/3] \sin[\pi/6 - (\alpha i - \delta - (ki-1)\pi/3)}{\sqrt{3}\cos(\delta)}$$

$$d2 = \frac{2q \sin[\alpha o - (kv-1)\pi/3] \sin[\pi/6 + (\alpha i - \delta - (ki-1)\pi/3)}{\sqrt{3}\cos(\delta)}$$

By similar analysis, the SCs selected to obtain V^{11}_o are +1(d_3) and −3 (d_4) with the following duty ratios:

$$d3 = \frac{2q \sin[kv^*\pi/3 - \alpha o] \sin[\pi/6 - (\alpha i - \delta - (ki-1)\pi/3)}{\sqrt{3}\cos(\delta)}$$

$$d4 = \frac{2q \sin[kv^*\pi/3 - \alpha o] \sin[\pi/6 + (\alpha i - \delta - (ki-1)\pi/3)}{\sqrt{3}\cos(\delta)}$$

Finally, zero SC (d_5) is applied to complete the sampling Period $d5 = 1 - (d1 + d2 + d3 + d4)$

$$d5 = 2q \cos[\alpha o - (2kv-1)\pi/6] \sin[\pi/6 + (\alpha i - \delta - (ki-1)\pi/3)$$

$\sqrt{3}\cos(\delta)$

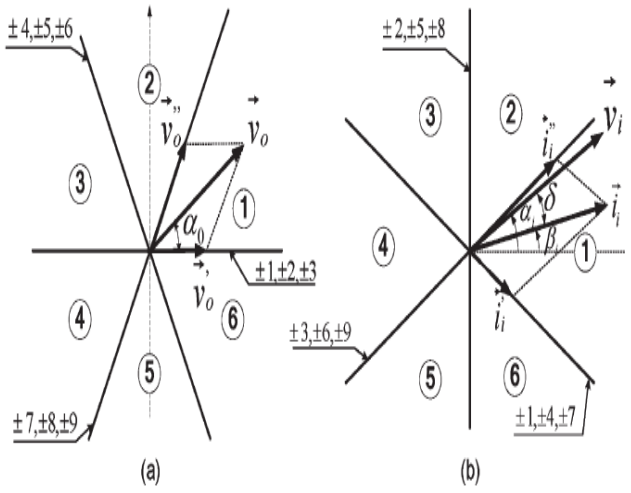

Fig. 3. (a) Output line-to-neutral voltage vector. (b) Input line current vector.

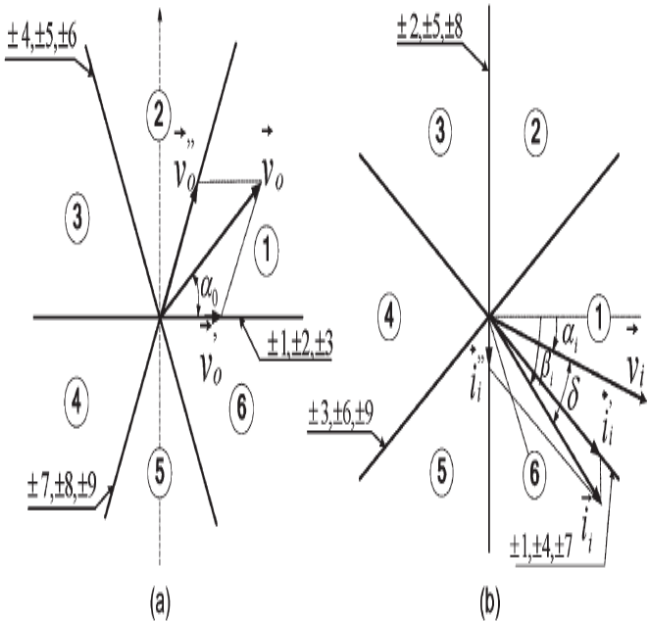

Fig. 4. (a) Output line-to-neutral voltage vector. (b) Input current and voltage vectors at different sectors.

where $d1$, $d2$, $d3$, $d4$, and $d5$ are the duty ratios of four active SCs (in this case, −7, +9, +1, and −3) and zero SC, respectively, and $q = vo/vm$ is the voltage transfer ratio. Table II shows all switching patterns that can be used in the DSVM method if the desired input current vector is located in the same sector with the input voltage vector.

Case 2: The displacement angle places the desired input current vector and input voltage vector in different sectors. Without missing the generality of the analysis, we assume that the input voltage vector is located in sector 1 ($-\pi/6 \le \alpha i \le \pi/6$) and that the desired input current vector is located in sector 6 ($-\pi/2 \le \beta i \le -\pi/6$) with the different phase angle δ shown in Fig. 4. Similar to Case 1, to generate the desired voltage vector _ vo and to maintain the desired different phase angle δ between the input current vector and the input voltage vector, the suitable SCs selected are −7, +8, +1, −2, and zero SCs with the following duty ratios:

$$d1 = \frac{2q \sin[\alpha o-(kv-1)\pi/3] \sin[\pi/6+(\alpha i-\delta-(ki-2)\pi/3)}{\sqrt{3}\cos(\delta)}$$

$$d2 = \frac{2q \sin[\alpha o-(kv-1)\pi/3] \sin[\pi/6-(\alpha i-\delta-(ki-2)\pi/3)}{\sqrt{3}\cos(\delta)}$$

$$d3 = \frac{2q \sin[kv*\pi/3 - \alpha o] \sin[\pi/6+(\alpha i-\delta-(ki-2)\pi/3)}{\sqrt{3}\cos(\delta)}$$

$$d4 = \frac{2q \sin[kv*\pi/3 - \alpha o] \sin[\pi/6-(\alpha i-\delta-(ki-2)\pi/3)}{\sqrt{3}\cos(\delta)}$$

$$d5 = \frac{2q \cos[\alpha o-(2kv-1)\pi/6] \sin[\pi/6+(\alpha i-\delta-(ki-2)\pi/3)}{\sqrt{3}\cos(\delta)}$$

where $d1$, $d2$, $d3$, $d4$, and $d5$ are the duty ratios of four active SCs (in this case, −7, +8, +1, and −2) and zero SC, respectively.

Table III shows all possible switching patterns if the desired input current vector and input voltage vector are located in different sectors.

C. Maximum Compensated Angle

The duty ratio of the zero SC has to be positive to validate the DSVM method. Considering the fact that $d5 \ge 0$, we obtain the following equation from above equations

$$q \le \sqrt{3}\cos(\delta)/2$$

From above equation the maximum voltage transfer ratio is inferred to be $\sqrt{3}\cos(\delta)/2$, and the well-known maximum voltage transfer ratio becomes $\sqrt{3}/2$ at $\delta = 0$.

TABLE II

Switching Patterns For The Input Voltage And Current Vectors Located In The Same Sector

Input voltage vetor sector	Output voltage vetor sector 1	2	3	4	5	6
1	-7 +9 +1 -3	+9 -8 -3 +2	-8 +7 +2 -1	+7 -9 -1 +3	-9 +8 +3 -2	+8 -7 -2 +1
2	+4 -6 -7 +9	-6 +5 +9 -8	+5 -4 -8 +7	-4 +6 +7 -9	+6 -5 -9 +8	-5 +4 +8 -7
3	-1 +3 +4 -6	+3 -2 -6 +5	-2 +1 +5 -4	+1 -3 -4 +6	-3 +2 +6 -5	+2 -1 -5 +4
4	+7 -9 -1 +3	-9 +8 +3 -2	+8 -7 -2 +1	-7 +9 +1 -3	+9 -8 -3 +2	-8 +7 +2 -1
5	-4 +6 +7 -9	+6 -5 -9 +8	-5 +4 +8 -7	+4 -6 -7 +9	-6 +5 +9 -8	+5 -4 -8 +7
6	+1 -3 -4 +6	-3 +2 +6 -5	+2 -1 -5 +4	-1 +3 +4 -6	+3 -2 -6 +5	-2 +1 +5 -4
Duty ratios	$d_1\ d_2\ d_3\ d_4$	$d_1\ d_2\ d_3\ d_4$	$d_1\ d_2\ d_3\ d_4$	$d_1\ d_2\ d_3\ d_4$	$d_1\ d_2\ d_3\ d_4$	$d_1\ d_2\ d_3\ d_4$

As seen from equation corresponding to each voltage transfer ratio q, there exists a possible maximum compensated displacement angle between the desired input current vector and the input voltage vector.

TABLE III

Switching Patterns For The Input Voltage And Current Vectors Located In The different Sector

Input voltage vetor sector	Output voltage vetor sector 1	2	3	4	5	6
1	-7 +8 +1 -2	+9 -7 -3 +1	-8 +9 +2 -3	+7 -8 -1 +2	-9 +7 +3 -1	+8 -9 -2 +3
2	+4 -5 -7 +8	-6 +4 +9 -7	+5 -6 -8 +9	-4 +5 +7 -8	+6 -4 -9 +7	-5 +6 +8 -9
3	-1 +2 +4 -5	+3 -1 -6 +4	-2 +3 +5 -6	+1 -2 -4 +5	-3 +1 +6 -4	+2 -3 -5 +6
4	+7 -8 -1 +2	-9 +7 +3 -1	+8 -9 -2 +3	-7 +8 +1 -2	+9 -7 -3 +1	-8 +9 +2 -3
5	-4 +5 +7 -8	+6 -4 -9 +7	-5 +6 +8 -9	+4 -5 -7 +8	-6 +4 +9 -7	+5 -6 -8 +9
6	+1 -2 -4 +5	-3 +1 +6 -4	+2 -3 -5 +6	-1 +2 +4 -5	+3 -1 -6 +4	-2 +3 +5 -6
Duty ratios	$d_1\ d_2\ d_3\ d_4$	$d_1\ d_2\ d_3\ d_4$	$d_1\ d_2\ d_3\ d_4$	$d_1\ d_2\ d_3\ d_4$	$d_1\ d_2\ d_3\ d_4$	$d_1\ d_2\ d_3\ d_4$

However, the new DSVM method is only validated if the input voltage vector leads the input current vector to one sector, i.e., $\delta \leq \pi/3$. The maximum compensated angle is given by

$$\boldsymbol{\delta}\max = \cos{-1}(\sqrt{2}q\backslash 3)\ ,\ \sqrt{3}\backslash 4 \leq q \leq \sqrt{3}\backslash 2$$

$$= \pi/3.\quad 0 < q \leq \sqrt{3}\,4\ .$$

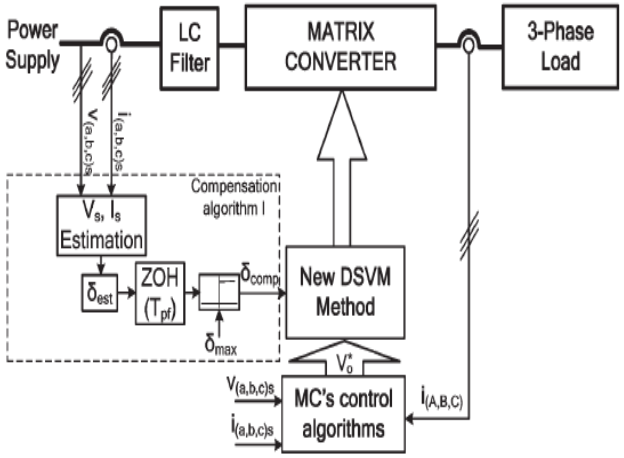

Fig. 5. Block diagram of compensation algorithm I based on the optimal compensated angle.

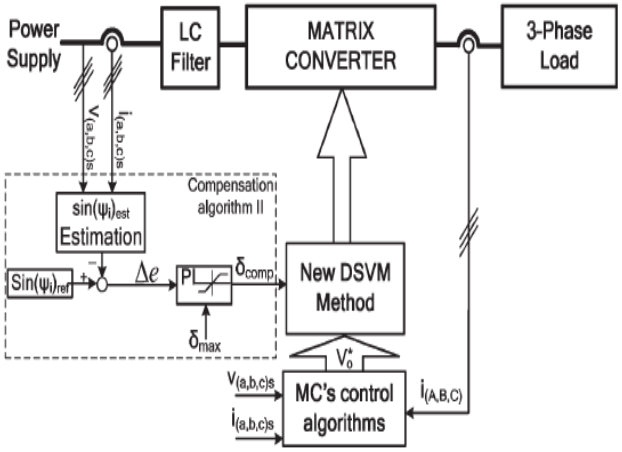

Fig. 6. Block diagram of compensation algorithm II based on the optimal compensated angle.

IPF COMPENSATION ALGORITHMS USING THE NEW DSVM METHOD

A. Compensation Algorithm Based on the Optimal Compensated Angle

From the filter characteristics explained in Section II, the main input current variation directly impacts the displacement angle between the main input phase voltage and the main input current.

To overcome this effect, a power factor compensation algorithm based on the optimal compensated angle (compensation algorithm I) is proposed. The optimal compensated angle is calculated in (8); its value depends on the main input current and main input voltage magnitudes, fundamental frequency, and LC values. Fig. 6 shows the proposed online block diagram. The compensated displacement angle is periodically updated at each compensating period T_{pf} (T_{pf} _ T_s), where T_s is the PWM sampling period.

The advantages of compensation algorithm I are as follows.

1) It improves the main power factor produced by the new DSVM method without changing the output control.

2) It reduces the main input current magnitude due to a smaller reactive power supply.

In compensation algorithm I, the estimation of the compensated angle is dependent on many parameters that impact on the accuracy of the optimal compensated angle estimation.

B. Compensation Algorithm Based on a PI Controller

To overcome the drawbacks in compensation algorithm I, another IPF compensation algorithm using a PI controller is proposed: compensation algorithm II.

In compensation algorithm II, a sine value of the displacement angle ϕi between the input line-to-neutral voltage vector and the corresponding input line current vector is chosen to control the IPF in Fig. 7. The unity power factor at the power supply side of the MC is intrinsically satisfied if the value of sin(ϕi) is maintained close to zero.

The proposed PI controller is noted by

$$\delta_{comp} = (Kp + Ki \backslash s)\Delta e$$

where

$$\Delta e = \sin(\phi i)_{ref} - \sin(\phi i)_{est}.$$

With this proposed algorithm, the compensating period required to maintain a high power factor is as the same as the PWM sampling period ($T_{pf} = T_s$). As the output changes, the PI still functions well in terms of the steady-state and dynamic performance achievement of the input side. Furthermore, this proposed algorithm is independent on the input filter and power supply parameters, which are quite sensitive during practical operations.

SIMULATION RESULTS:

Simulation was carried out on a three-phase RL load using Matlab software. The simulation parameters for the RL load were as follows:

1) power supply (line-to-neutral voltage): 100 V/60 Hz;

2) three-phase RL load: 26 Ω, 12 mH.

The input filter was designed with L = 1. 4 mH, C = 22. 5 μF, and Y connection. The PWM frequency was 10 kHz, and simulation results were obtained under a constant V/f condition. Fig. 7 (a) shows the simulation results of the conventional DSVM method at reference output voltage q = 0. 7, f_o = 70 Hz. The input current of the MC is in phase with the input line-to-neutral voltage. However, the main power supply current lags behind the input line-to-neutral voltage due to the input low-pass filter, as explained in Section II. The IPF obtained here is only 0.912 shows in fig 7(b).

In order to determine the differences between the conventional DSVM method and our new DSVM method, the same reference output voltage was applied using compensation algorithm II shown in Fig. 8. Due to the optimal compensated angle achieved by the PI controller, the main input current at the power supply is in phase with the line-to-neutral input voltage, while the MC satisfies the reference output voltage presented inthe figure by the output currents and line-to-line output voltage. Fig. 9(a)–(b) shows the steady-state performances at reference output voltage q = 0. 4, f_o = 40 Hz of the conventional DSVM method, compensation algorithm I, and compensation algorithm II, respectively.

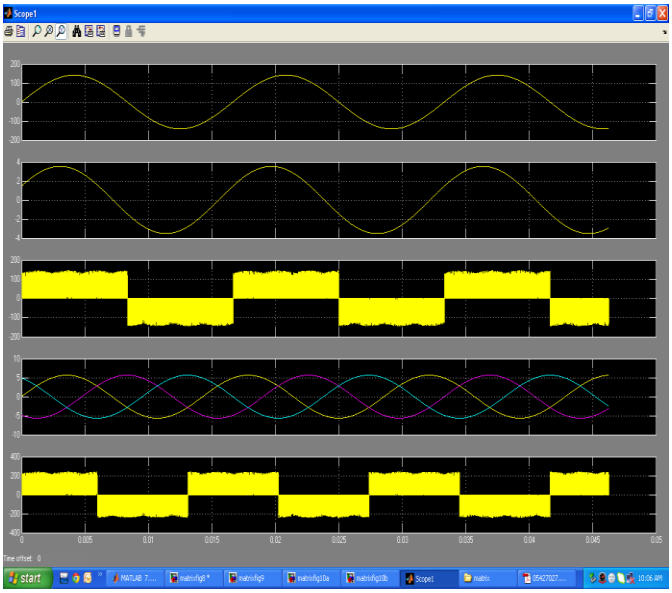

Fig 7. Input/output waveforms of the MC at reference output voltage q = 0.7, f_o = 70 Hz with the conventional DSVM method (pf = 0.912).

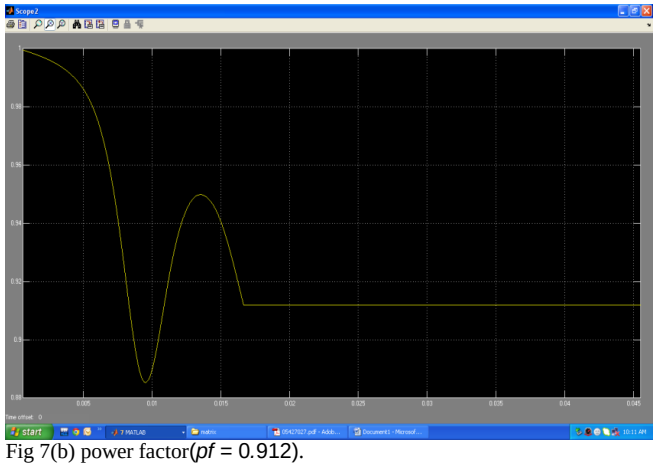

Fig 7(b) power factor(pf = 0.912).

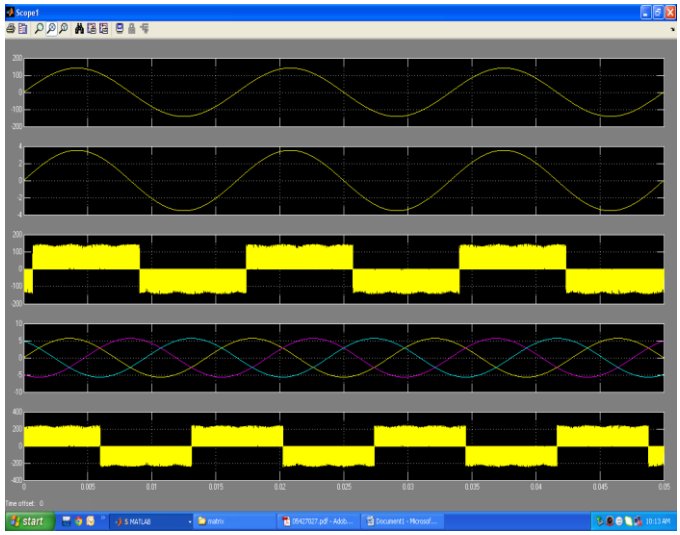

Fig.8(). Input/output waveforms of the MC at reference output voltage q = 0.7, f_o = 70 Hz with compensation algorithm II (pf = 1.0).

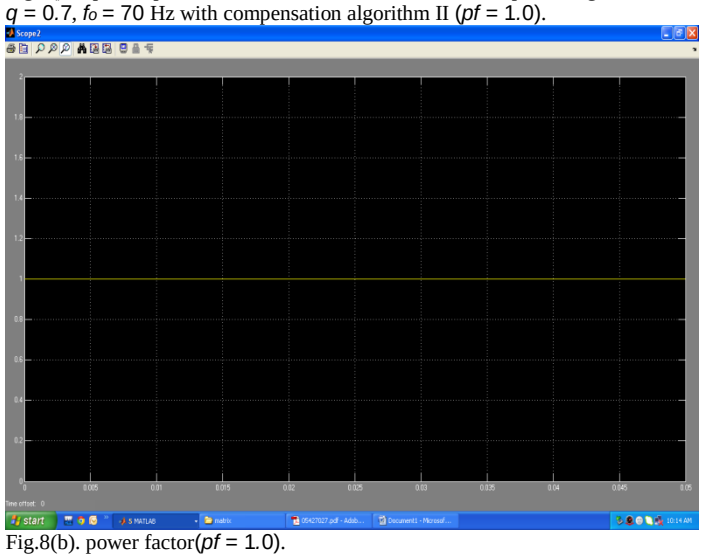

Fig.8(b). power factor(pf = 1.0).

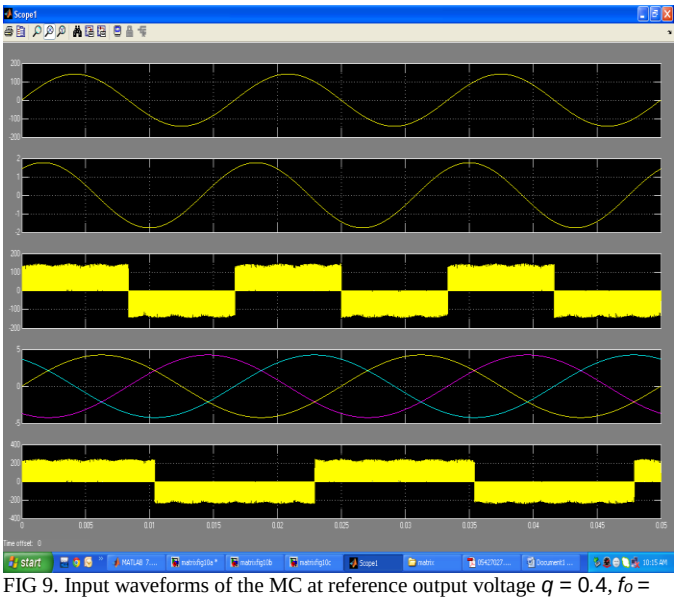

FIG 9. Input waveforms of the MC at reference output voltage q = 0.4, f_o = 40 Hz. (a) Conventional DSVM method

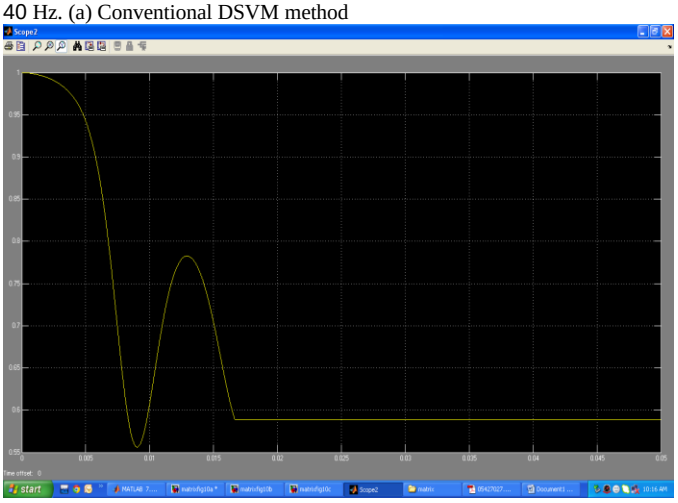

Power factor=(pf = 0.589)

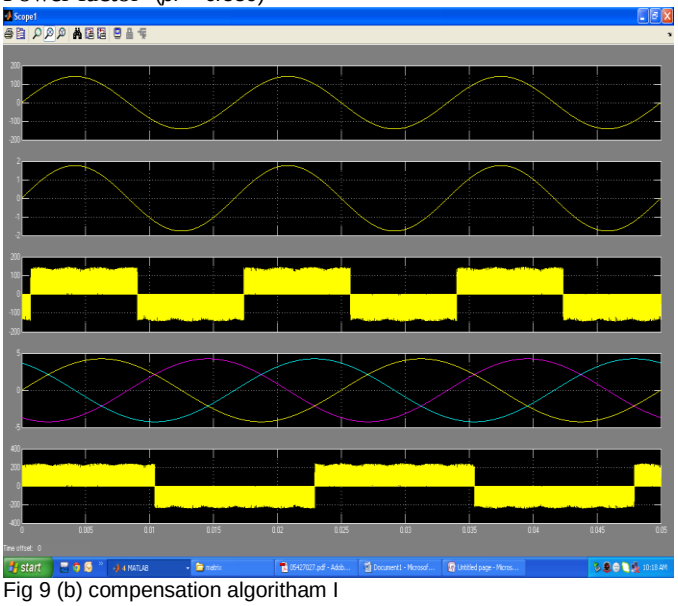

Fig 9 (b) compensation algoritham I

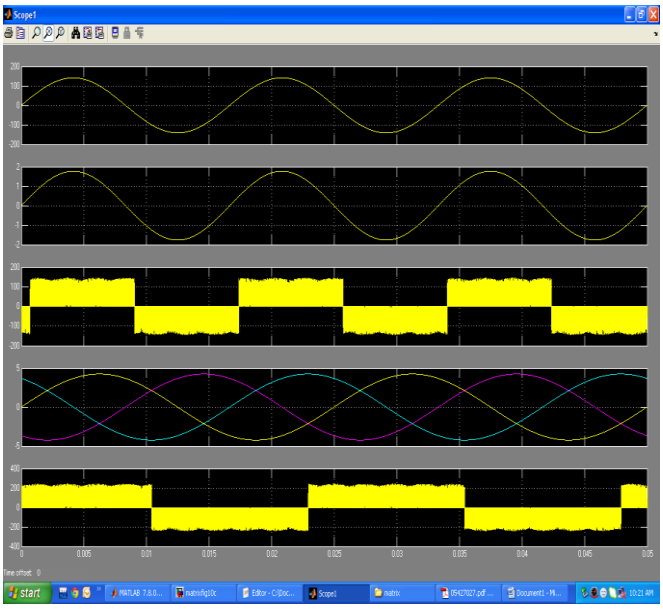

FIG 9:Input waveforms of the MC at reference output voltage $q = 0.4$, $f_o = 40$ Hz (c) Compensation algorithm II ($pf = 1.0$).

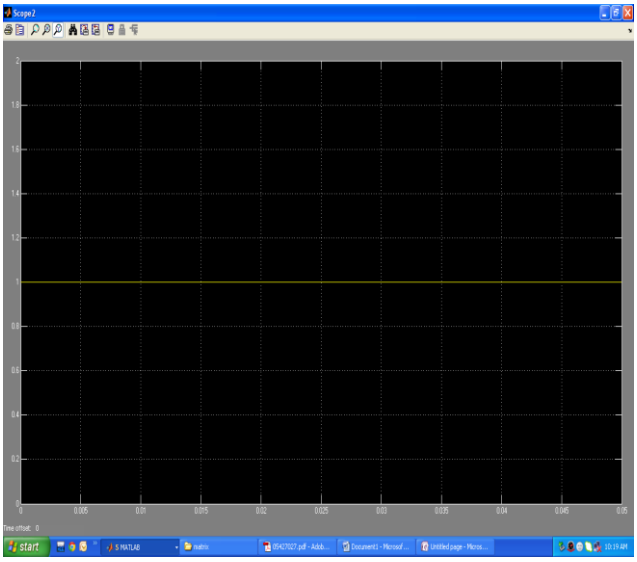

FIG 9(C)POWER FACTOR = 1 WITH Compensation algorithm II.

The input currents and voltage waveforms in Fig. 10(a) present the IPF at 0.589. The input currents and voltage waveforms in Fig. 10(b) and (c) describe the MC operations with the optimal compensated angle for compensation algorithms I and II, respectively. The power factors for both algorithms are achieved at unity.FIG 9 (C) shows that the cosine of angle between supply voltage and current is unity so power factor with compensation algoritham II is unity.

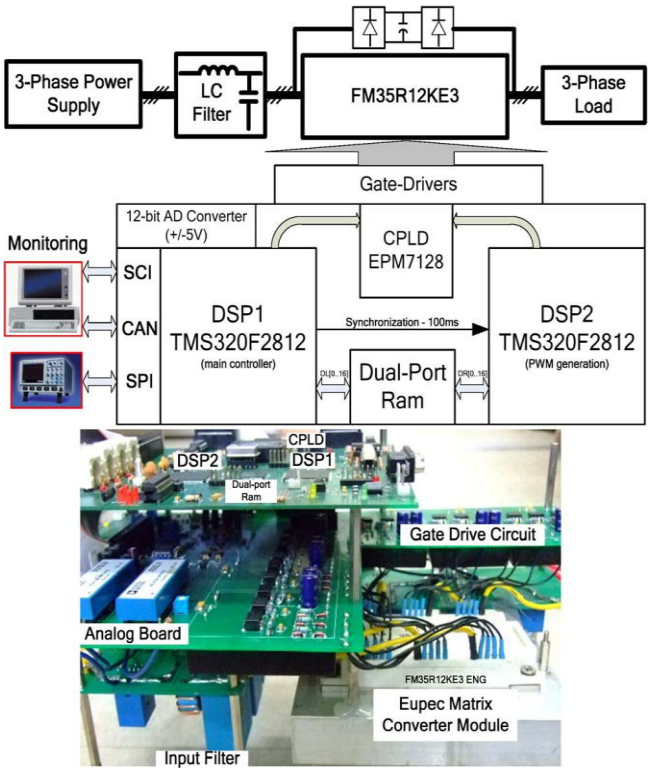

FIG 10.Block diagram of the MC hardware configuration and laboratory MC prototype.

VII. CONCLUSION:

We have proposed a new DSVM method for MC with the goal of achieving an IPF of unity on the main power supply side. The operational principle of the new DSVM method was presented based on the analyses of the maximum allowable compensated angle, and a new PWM switching pattern was also introduced. The new DSVM method was realized by the two proposed IPF compensation algorithms. In addition to the high input power region being enlarged significantly, the smaller input current magnitude was obtained by utilizing the minimum reactive power supply. Comparison of performances between the two algorithms was carried out and explained in details. The steady-state and transient responses of the proposed algorithms were tested through both simulation and experiment using the three-phase *RL* load model.

REFERENCES:

[1] E.Watanabe, S. Ishii, E. Yamamoto, H. Hara, J.-K. Kang, and A.M. Hava, "High performance motor drive using matrix converter," in *Proc. IEE Seminar Adv. Induction Motor Control (Ref. No. 2000/072)*, May 2000, pp. 711–716.

[2] C. Klumpner, P. Nielsen, I. Boldea, and F. Blaabjerg, "A new matrix converter motor (MCM) for industry applications," *IEEE Trans. Ind. Electron.*, vol. 49, no. 2, pp. 325–335, Apr. 2002.

[3] T. F. Podlesak, D. C. Katsis, P. W. Wheeler, J. C. Clare, L. Empringham, and M. Bland, "A 150-kVA vector-controlled matrix converter induction motor drive," *IEEE Trans. Ind. Appl.*, vol. 41, no. 3, pp. 841–847, May/Jun. 2005.

[4] P. W. Wheeler, J. Rodriguez, J. C. Clare, L. Empringham, and

A.Weinstein, "Matrix converters: A technology review," *IEEE Trans. Ind. Electron.*, vol. 49, no. 2, pp. 276–288, Apr. 2002.
[5] P. W. Wheeler, H. Zhang, and D. A. Grant, "A theoretical, and practical consideration of optimised input filter design for a low loss matrix converter," in *Proc. 9th Int. Conf. Electromagn. Compat.*, Sep. 1994, pp. 138–142.
[6] P. Wheeler and D. Grant, "Optimized input filter design, and low-loss switching techniques for a practical matrix converter," *Proc. Inst. Elect. Eng.—Elect. Power Appl.*, vol. 144, no. 1, pp. 53–60, Jan. 1997.
[7] D. Casadei, G. Serra, A. Tani, and L. Zarri, "Stability analysis of electrical drives fed by matrix converters," in *Proc. IEEE ISIE*, Jul. 2002, vol. 4, pp. 1108–1113.
[8] D. Casadei, G. Serra, A. Tani, and L. Zarri, "Effects of input voltage measurement on stability of matrix converter drive system," *Proc. Inst. Elect. Eng.—Elect. Power Appl.*, vol. 151, no. 4, pp. 487–497, Jul. 2004.
[9] D. Casadei, G. Serra, A. Tani, A. Trentin, and L. Zarri, "Theoretical, and experimental investigation on the stability of matrix converters," *IEEE Trans. Ind. Electron.*, vol. 52, no. 5, pp. 1409–1419, Oct. 2005.
[10] D. Casadei, J. Clare, L. Empringham, G. Serra, A. Tani, P. W. Wheeler, and L. Zarri, "Large-signal model for the stability analysis of matrix converters," *IEEE Trans. Ind. Electron.*, vol. 54, no. 2, pp. 939–950, Apr. 2007.
[11] J. Wang and M. Bouazdia, "Influence of filter parameters/topologies on stability of matrix converter-fed permanent magnet brushless motor drive systems," in *Proc. IEEE Int. Elect. Machines and Drives Conf.*,May 2009, pp. 964–970.
[12] S. F. Pinto and J. F. Silva, "Input filter design for sliding mode controlled matrix converters," in *Proc. 32nd IEEE Annu. Power Electron. Spec. Conf.*, Jun. 2001, vol. 2, pp. 648–653. NGUYEN *et al.*: INPUT POWER FACTOR COMPENSATION ALGORITHMS USING A NEW DSVM METHOD FOR MC 243
[13] S. F. Pinto and J. F. Silva, "Direct control method for matrix converters with input power factor regulation," in *Proc. 35th IEEE Power Electron. Spec. Conf.*, Jun. 2004, vol. 3, pp. 2366–2372.
[14] K. Yamada, T. Higuchi, E. Yamamoto, H. Hara, T. Sawa, M. M. Swamy, and T. Kume, "Filtering techniques for matrix converters to achieve environmentally harmonics drives," in *Proc. 11th EPE*, Dresden, Germany, 2005.
[15] H.-H. Lee, H. M. Nguyen, and T.-W. Chun, "New direct-SVM method for matrix converter with main input power factor compensation," in *Proc. 34th IEEE IECON*, Nov. 10–13, 2008, pp. 1281–1286.

Malgireddy Ravi **was** born in Ramapuram, Nalgonda dist, in A.P in 1982. He received the B.Tech. Degree in electrical engineering from J.N.T University, Hyderabad In 2005 with Distinction Class. He received master of technology (M.Tech) in embedded system with Distinction Class. He is currently with the Blue Vega Solutions Pvt.Ltd Hyderabad as Technical Manager for electrical. His research interests are electrical drives, industrial networks, renewable energy, and modern power converters and solar power generation.

Palarapu Sravan Kumar palarapu sravan kumar born in kalvalapally village nalgonda district in year 1987(14 may) i received B.Tech degree in Electrical engineering 2008 from SV engineering college suryapet with first class, i recieved M.Tech in power electronics with distriction form Gokaraju rangarju institute of engg & technology hyderabad in 2011 and my area of interest are FACTS and power quality.